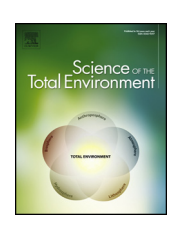
EISEVIED

Contents lists available at ScienceDirect

Science of the Total Environment

journal homepage: www.elsevier.com/locate/scitotenv



Metalimnetic oxygen minima alter the vertical profiles of carbon dioxide and methane in a managed freshwater reservoir



Ryan P. McClure ^{a,*}, Kathleen D. Hamre ^a, B.R. Niederlehner ^a, Zackary W. Munger ^b, Shengyang Chen ^c, Mary E. Lofton ^a, Madeline E. Schreiber ^b, Cayelan C. Carey ^a

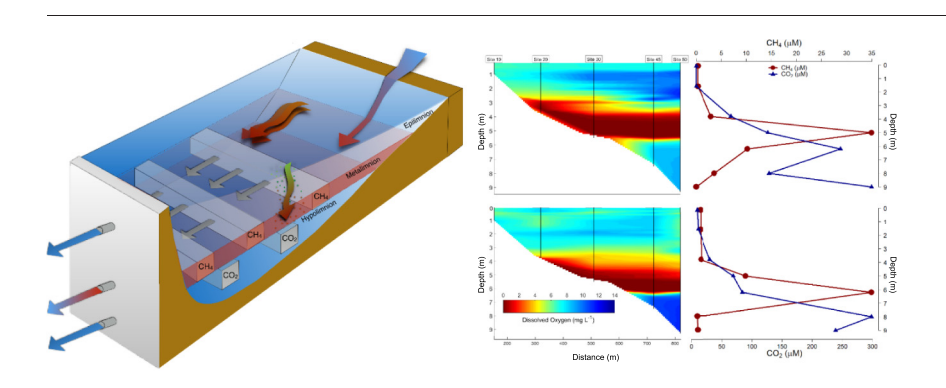
- ^a Department of Biological Sciences, Virginia Tech, Blacksburg, VA 24061, USA
- ^b Department of Geosciences, Virginia Tech, Blacksburg, VA 24061, USA
- ^c School of Civil Engineering, University of Sydney, Sydney, NSW 2006, Australia

HIGHLIGHTS

Metalimnetic oxygen minimum zones (MOMs) commonly develop in freshwater reservoirs.

- Dissolved greenhouse gases and emissions were monitored in a reservoir with MOMs
- MOMs altered the seasonal profiles of CH₄ and CO₂ in the water column.
- Methane (CH₄) accumulated in the MOMs that developed both monitoring periods.
- Evaluation of MOMs on GHGs is critical as reservoir construction increases.

GRAPHICAL ABSTRACT



ARTICLE INFO

Article history: Received 28 January 2018 Received in revised form 6 April 2018 Accepted 19 April 2018 Available online xxxx

Editor: José Virgílio Cruz

Keywords:
Diffusive emissions
Greenhouse gases
Oxygen minimum zone
Redox gradient
Reservoirs
Water quality management

ABSTRACT

Metalimnetic oxygen minimum zones (MOMs) commonly develop during the summer stratified period in freshwater reservoirs because of both natural processes and water quality management. While several previous studies have examined the causes of MOMs, much less is known about their effects, especially on reservoir biogeochemistry. MOMs create distinct redox gradients in the water column which may alter the magnitude and vertical distribution of dissolved methane (CH₄) and carbon dioxide (CO₂). The vertical distribution and diffusive efflux of CH₄ and CO₂ was monitored for two consecutive open-water seasons in a eutrophic reservoir that develops MOMs as a result of the operation of water quality engineering systems. During both summers, elevated concentrations of CH₄ accumulated within the anoxic MOM, reaching a maximum of 120 μ M, and elevated concentrations of CO₂ accumulated in the oxic hypolimnion, reaching a maximum of 780 μ M. Interestingly, the largest observed diffusive CH₄ effluxes occurred before fall turnover in both years, while peak diffusive CO₂ effluxes occurred both before and during turnover. Our data indicate that MOMs can substantially change the vertical distribution of CH₄ and CO₂ in the water column in reservoirs, resulting in the accumulation of CH₄ in the metalimnion (vs. at the sediments) and CO₂ in the hypolimnion.

© 2018 Elsevier B.V. All rights reserved.

1. Introduction

Human-made reservoirs are major contributors of diffusive carbon dioxide (CO₂) and methane (CH₄) effluxes to the atmosphere (Deemer et al., 2016). Despite their small global surface area relative

E-mail address: ryan333@vt.edu (R.P. McClure).

 ^{*} Corresponding author at: 1000 Derring Hall, 926 West Campus Drive, Blacksburg, VA 24061, USA.

to naturally-formed lakes (Downing et al., 2006), reservoirs may contribute up to 36.8 Tg $\rm CO_2~yr^{-1}$ and 13.3 Tg $\rm CH_4~yr^{-1}$ to the atmosphere, representing approximately 1.3% of gross anthropogenic $\rm CO_2$ equivalent emissions (Deemer et al., 2016). Reservoir construction is increasing globally to satisfy the demands for renewable energy, agriculture, and drinking water (Zarfl et al., 2015); thus, determining the factors that control the magnitude of diffusive $\rm CO_2$ and $\rm CH_4$ efflux from reservoirs is critical for constraining the global carbon (C) budget (Cole et al., 2007; Tranvik et al., 2009).

Reservoir CO_2 and CH_4 dynamics are controlled in part by dissolved oxygen (DO) concentrations in the water column and at the sediments. Many reservoirs exhibit anoxic hypolimnia (DO concentrations <0.5 mg L^{-1}) that accumulate high concentrations of CH_4 during the summer stratified period. As a result, peak diffusive CH_4 efflux in these reservoirs generally occurs on the day of fall turnover when the CH_4 in the anoxic hypolimnion reaches the upper mixed layer (e.g., Musenze et al., 2014; Rasilo et al., 2015). As CH_4 diffuses upward through the water column to the surface during turnover, most of it will be oxidized to CO_2 upon contact with oxic waters, resulting in peak CO_2 diffusive efflux rates during turnover as well (Bastviken et al., 2004).

In contrast to reservoirs that develop anoxic hypolimnia, some reservoirs instead develop metalimnetic oxygen minima (MOMs), or zones of depleted DO in the middle of the water column (Thornton et al., 1990), which may affect CH_4 and CO_2 vertical profiles. In a review of the literature, we identified 40 reservoirs in which MOMs were reported (Appendix 1, Table I), or a MOM was observed in a figure but not reported explicitly in the text (Appendix 2, Table I). Many of these reservoirs developed MOMs during the stratified period and were managed with engineered systems used to improve water quality. An analysis of the morphometric characteristics of these reservoirs suggests that MOMs can form in a wide range of varying-sized reservoirs (Table 1).

MOMs can form in reservoirs due to both natural processes and human management. Several natural processes were identified as drivers of MOMs in the literature review, including the lateral entrainment of low-oxygen or nutrient and organic-rich water from inflows that stimulates microbial respiration in the metalimnion (Effler et al., 1998; Joehnk and Umlauf, 2001; Shapiro, 1960; Bolke, 1979); and settling of organic matter from the surface that slows at the thermocline and is consumed, subsequently depleting DO (Kreling et al., 2017; Thornton et al., 1990). In addition to natural processes, water that is discharged from a reservoir's dam at a depth that corresponds with the thermocline can exacerbate the development of a MOM in reservoirs by increasing the internal flows that entrain upstream nutrients toward the intake (Williams, 2007).

Water quality management systems that are commonly deployed in reservoirs, such as hypolimnetic oxygenation (HOx) and epilimnetic mixing (EM) systems, also promote the development of MOMs (Gerling et al., 2014; Chen et al., 2017, 2018). HOx systems can result in MOMs when laterally-entrained low-oxygen water depletes DO conditions in the metalimnion (Chen et al., 2017, 2018), and the hypolimnion is successfully oxygenated due to HOx operation (reviewed by Gerling et al., 2014). HOx systems can also generate a MOM if they are unable to oxygenate the entire hypolimnion, leaving low DO water just below the thermocline (e.g., Gerling et al., 2014). Similarly, operation of EM systems can increase the lateral entrainment of nutrient-

rich turbid water from shallow upstream regions to the reservoir's metalimnion in the lacustrine zone (Munger et al., 2016; Chen et al., 2017, 2018).

The development of MOMs may create redox gradients within the water column that affect the vertical distribution of CO_2 and CH_4 in the water column and the magnitude and timing of diffusive efflux. For example, if a MOM becomes anoxic, it may accumulate elevated concentrations of CH_4 in the middle of the water column instead of the hypolimnion. Moreover, MOMs may also alter the timing of peak CH_4 and CO_2 emissions. If CH_4 is present in a MOM, deeper mixing into the water column due to storms or other disturbances could entrain low-oxygen metalimnetic water to the surface, thereby resulting in increased CH_4 and CO_2 diffusive effluxes before turnover.

We conducted a whole-reservoir monitoring study to examine how MOMs in reservoirs affect CH₄ and CO₂ water column concentrations and diffusive CH₄ and CO₂ emissions during two consecutive summers. MOMs were developed by operating a HOx and EM system in a eutrophic drinking water reservoir that has previously exhibited MOMs (Chen et al., 2017; Gerling et al., 2014, 2016; Munger et al., 2016) during the open-water seasons of 2015 and 2016. The EM system was operated independently from the HOx to stimulate lateral entrainment of nutrients from upstream and to further promote the development of the MOM (following Chen et al., 2018). HOx and EM systems are increasingly being used to suppress hypolimnetic anoxia and algae blooms in lakes and reservoirs globally (Chen et al., 2017; Liboriussen et al., 2009; Singleton et al., 2010; Beutel and Horne, 1999); however, to our knowledge there are no studies that specifically investigate the effects of HOx and EM operation on MOMs and their consequences for greenhouse gas (GHG) dynamics.

Throughout the whole-reservoir monitoring study, we measured the effects of the MOMs on the vertical profiles of CO₂ and CH₄ in the water column and diffusive CH₄ and CO₂ effluxes. We predicted that CH₄ would accumulate in the MOM after it had become anoxic, in comparison to CO₂, which would accumulate in the oxygenated hypolimnion because of HOx operation and increased aerobic respiration rates at the sediments. We also predicted that any CH₄ that accumulated in the MOM would result in increased CH₄ diffusive effluxes if strong winds or mixing events occurred during summer stratified conditions, decoupling the timing of peak diffusive effluxes from fall turnover. In contrast, CO₂ diffusive efflux was predicted to peak during turnover because CO₂ accumulated in the hypolimnion would not be able to reach the upper mixed layer until the entire water column mixed at the end of the summer stratified period (following Vachon and del Giorgio, 2014).

2. Materials and methods

2.1.1. Site descriptions

The whole-reservoir manipulations to generate and monitor MOMs were conducted in Falling Creek Reservoir (FCR). FCR is a small (surface area = 0.119 km²), shallow ($Z_{\rm max} = 9.3$ m, $Z_{\rm mean} = 4.0$ m), eutrophic, drinking water reservoir located in Vinton, Virginia, USA (37.30°N, 79.84°W) (Fig. 1). The reservoir was constructed in 1898 and is owned by the Western Virginia Water Authority (WVWA) and has one primary inflow stream from an upstream reservoir that contributes

Table 1Summary statistics of morphometric characteristics of reservoirs that have reported or observed but not explicitly reported MOMs. S.E. refers to standard error of the mean; S.D. refers to standard deviation of the mean.

	Volume (km³)	Maximum depth (m)	Minimum depth (m)	Surface area (km²)	Perimeter (km)	Catchment area (km²)	Elevation (m)
Mean	3.2	73	34	85	370	32,000	540
Median	0.7	58	25	44	240	4000	340
Minimum	0.01	9.0	3	0.4	4.0	7.0	27
Maximum	37	200	210	650	3800	420,000	2300
S.E. mean	1.3	9.3	7.4	25	120	14,000	98
S.D. mean	7.5	50	38	140	670	85,000	560

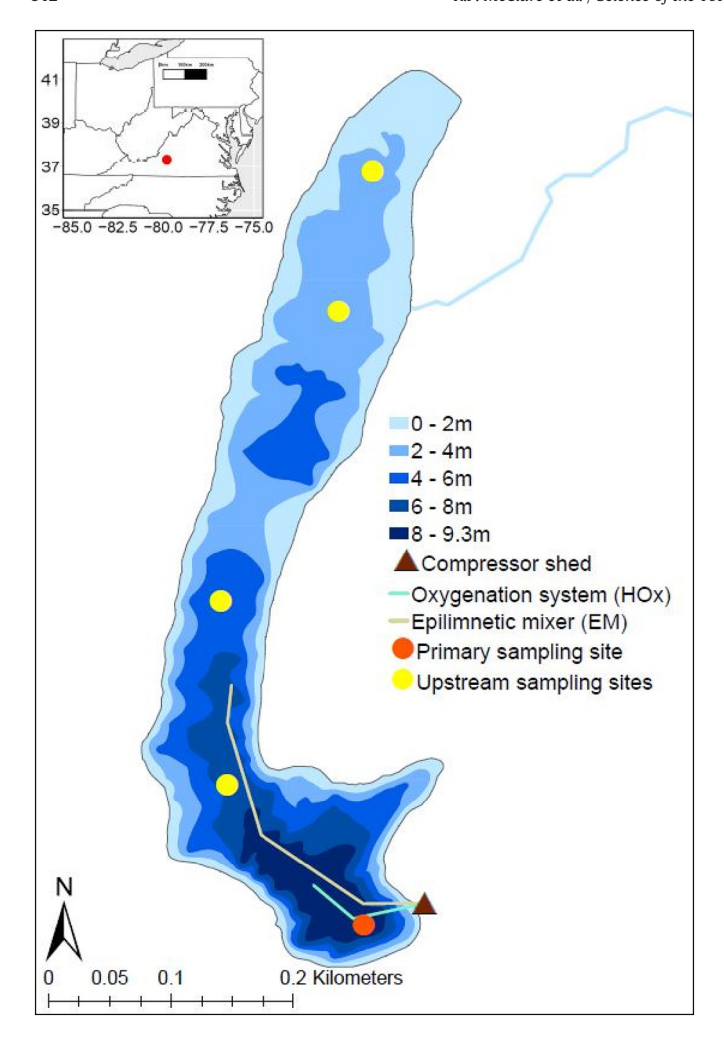


Fig. 1. Bathymetry map of FCR and the five reservoir sampling sites. All water chemistry data were collected at the primary sampling site (red dot) and additional dissolved oxygen and temperature profiles were collected at upstream sites (yellow dots). (For interpretation of the references to colour in this figure legend, the reader is referred to the web version of this article.)

the majority of the water into the reservoir (Gerling et al., 2016). FCR is a dimictic reservoir and is thermally stratified generally between April to October (Gerling et al., 2016; Munger et al., 2016).

2.1.2. Hypolimnetic oxygenation (HOx) and epilimnetic mixing (EM) systems

In 2012, the WVWA deployed a side stream supersaturation HOx system and a bubble plume EM system in FCR to improve the water quality (Gerling et al., 2016, 2014; Munger et al., 2016). The HOx increases DO concentrations just above the sediments in the hypolimnion by pumping hypolimnetic water onshore to an oxygen saturation chamber, where 95% pure oxygen gas is dissolved into the water. The supersaturated water is pumped back into the hypolimnion at the same depth from where it was extracted and is mixed throughout the entire hypolimnion while not disrupting thermal stratification or water temperature (Gerling et al., 2014). The well-oxygenated hypolimnion due to HOx operation prevents the release of reduced metals and nutrients from the sediments (Gerling et al., 2014; Munger et al., 2016). The EM injects bubbled air into the epilimnion and upper metalimnion of FCR to mix the surface waters and decrease cyanobacterial blooms (Chen et al., 2017, 2018). When the EM is deactivated, operation of the HOx strengthens the thermocline and thermal stratification of the reservoir, generating suitable conditions for organic carbon decomposition and the entrainment of inflowing low DO water from the sediments to create MOMs at the thermocline. The HOx is generally activated through the entire summer stratified period in FCR, while the EM is only activated intermittently as needed.

MOMs have formed in FCR in all summers during the operation of both engineered systems (Chen et al., 2017; Gerling et al., 2016, 2014; Munger et al., 2016). The HOx and EM can be operated independently to develop MOMs in FCR, which allowed us to examine the $\rm CO_2$ and $\rm CH_4$ dynamics in the presence of MOMs in the reservoir. For a detailed description of the HOx system, refer to Gerling et al. (2014), and for a detailed description of the EM system, refer to Chen et al. (2018).

2.1.3. HOx and EM operation

The HOx and EM were operated to create MOMs in FCR throughout the monitoring periods of 2015 and 2016 (Table 2) in collaboration with the WVWA. The HOx was activated each spring when DO reached ~50% saturation at the sediments and was operated almost continuously until one month after turnover. The EM was activated both summers using short aeration pulses to mix the epilimnion and upper metalimnion to stimulate the lateral entrainment of upstream organic nutrients into the pelagic zone of FCR. The engineered systems' operation allowed us to create distinct MOMs and strong redox gradients in the water column during the monitoring period.

The HOx system was operated throughout both summer stratified periods to develop MOMs for studying water column CO₂ and CH₄ dynamics. The oxygen addition rate to the hypolimnion in all the activation periods varied between 12.5 and 20 kg d⁻¹, with a recycled flow rate during oxygenation periods of 227 L min⁻¹ (Table 2). At this flow rate, the total hypolimnetic volume was circulated through the HOx every 20–30 days. In 2015, from 5 May to 20 November, the HOx was activated to maintain suitable conditions for water treatment, except for a one-week interval in June and a 1.5 h interval on 28 July (Table 2). In 2016, the HOx was operated from 18 April through 11 November, and the oxygen addition rate also varied between 12.5 and 20 kg O₂ d⁻¹, with the same recycled flow rate as 2015 (227 L min⁻¹; Table 2). The HOx remained activated throughout the entire stratification period in 2016.

2.1.4. Field and laboratory data collection

We monitored the physical and chemical conditions in FCR to determine how CO_2 and CH_4 dynamics responded to the presence of MOMs. Depth profiles for temperature and DO concentrations were measured using a SBE 19 plus CTD profiler (Seabird Electronics, Bellevue, WA, USA) coupled with a SBE 43 DO sensor. The CTD and SBE 43 sensors were calibrated to the manufacturer's specifications at Seabird Electronics annually before each monitoring season. CTD profiles were collected at the deep hole and four upstream sites (Fig. 1) to compare conditions along the reservoir continuum. Temperature profiles were used to

Table 2Schedule and magnitude of oxygen and air addition from the hypolimnetic oxygenation system (HOx) and epilimnetic mixer (EM) during the monitoring periods in 2015 and 2016. Dates not listed below were days when both the HOx and the EM were not in use.

Dates of activation	O ₂ addition rate (kg d ⁻¹)	Air addition rate (kg d^{-1})
5 May – 1 June 2015 (HOx)	15	0
1 June 2015 (3 h) (EM)	0	1.02×10^{6}
3 June 2015 (4 h) (EM)	0	1.02×10^{6}
8 June – 23 June 2015 (HOx)	12.5	0
22-24 June 2015 (48 h) (EM)	12.5	4.07×10^{5}
23 June – 27 July 2015 (HOx)	20	0
28 July - 8 August 2015 (HOx)	15	0
8 August – 20 November 2015 (HOx)	20	0
18 April – 11 November 2016 (HOx)	15-20	0
25 May 2016 (6 h) (EM)	0	1.02×10^{6}
27 June – 28 June (24 h) 2016 (EM)	0	4.4×10^5
25 July – 27 July (48 h) 2016 (EM)	0	$2.05 \times 10^5 - 1.02 \times 10^6$

calculate thermocline depths and the depths of the top and bottom of the metalimnion for each sample date using rLakeAnalyzer (Read et al., 2011), a package in the R statistical environment (R Core Team, 2016). Fall turnover was determined as the day that the temperature at 1 m equaled the temperature at 8 m using observations collected every 15 min throughout the monitoring period by two optical INW DO2 DO sondes (Seametrics, South Kent, WA, USA).

From March through November in both years, we measured weekly depth profiles of CH_4 and CO_2 concentrations in the water column. Water samples were collected with a 4-L Van Dorn sampler (Wildlife Supply Co., Yulee, FL, USA) at seven depths (0.1, 1.6, 3.8, 5.0, 6.2, 8.0, and 9.0 m) at the deepest site in the reservoir. Water samples for CH_4 and CO_2 analysis were transferred from the Van Dorn sampler into replicate 20-mL serum vials using gravity flow through a tube, overflowing the vials. The vials were immediately capped without headspace and kept on ice until analysis within 24 h. Volume-weighted CH_4 and CO_2 concentrations were calculated by summing each greenhouse gas depth concentration multiplied by the volume of its corresponding layer from the bathymetry map (Fig. 1) and then dividing this value by the total volume in the water column.

Standard methods from the U.S. EPA method RSKSOP-175 (Hudson, 2004) were adapted to generate headspace in the samples and determine the dissolved concentrations of CO₂ and CH₄ in the water column. At the time of analysis, a 2-mL helium (He) headspace was created by displacing 2-ml of water with He in a closed system using two syringes simultaneously. The 2-mL headspace was equilibrated with the water sample by shaking the 20-mL serum vials at 300 rpm for 15 min at room temperature. After the samples were equilibrated, the 2-mL headspace in the sample vials were injected into a gas chromatograph (GC; SRI, model 8010) equipped with a flame ionization detector (FID) and thermal conductivity detector (TCD). The oven temperature in the GC was 35 °C and the carrier gas used for the separation was He with a flow rate of 15 mL min⁻¹. The retention times for CH₄ on FID and CO₂ on TCD were 1.3 and 2.8 min, respectively. Dissolved CO2 and CH4 concentrations in the water were back-calculated from the observed headspace concentrations using Henry's law (Sander, 2015). The median relative percent difference between replicate determinations of dissolved concentrations was 8.3 and 11.2% for CH₄ and CO₂, respectively.

2.1.5. CO₂ and CH₄ diffusive efflux

We calculated the diffusive CO_2 and CH_4 efflux from the surface of FCR into the atmosphere for each day CO_2 and CH_4 samples were collected. The concentrations of the CO_2 and CH_4 samples collected at the reservoir's surface (0.1 m) were applied to the surface diffusive efflux equation to determine the efflux at the time of collection:

$$Flux = k \times ([C_{surf}] - [C_{air}]) \tag{1}$$

where k is the gas transfer velocity or piston velocity (m d⁻¹), the depth of the water column that equilibrates with the atmosphere over time (Wanninkhof, 1992), and C_{surf} and C_{air} are the concentrations of CO_2 and CH_4 at the reservoir surface and the atmosphere directly above the water surface, respectively.

The *k* value that corresponded with each sampling day was calculated with the LakeMetabolizer package in R (Winslow et al., 2016), using the *U*10 corrected daily mean wind speed and air temperature measured from the Roanoke Airport in 2015 (~11 km from FCR), and a meteorological station deployed on FCR's dam in 2016. The Cole model (Cole et al., 2010) within the LakeMetabolizer package was used because it is considered a conservative model to calculate *k* among piston velocity models (Dugan et al., 2016). The 2015 atmospheric concentrations of CO₂ were measured at an eddy-flux covariance tower at the Tilden Meyers AmeriFlux US-WBW Walker Branch Watershed, Oak Ridge National Laboratory, Oak Ridge, Tennessee, USA (AmeriFlux BASE Dataset; https://ameriflux.lbl.gov), the closest site with available atmospheric CO₂ concentrations that represented a

similar land cover to FCR's forested watershed and the national average atmospheric CH₄ concentrations from the Carbon Dioxide Information Analysis Center (http://cdiac.ornl.gov/pns/current_ghg.html) as our atmospheric CH₄ concentrations. In 2016, air samples were collected above the water's surface in the serum vials and sealed with a crimper to calculate the ambient CH₄ and CO₂ atmospheric concentrations.

3. Results

3.1. Seasonal characteristics

3.1.1. Inflow and precipitation dynamics

FCR exhibited slightly different inflow rates and precipitation totals between the 2015 and 2016 seasons. FCR received ~258 mm of precipitation during the 2015 monitoring season (31 March – 7 December 2015) and ~197 mm during the 2016 season (30 March – 11 November 2016). The mean inflow rate of the primary inflow into FCR was 0.05 \pm 0.03 (1 S.D.) m³ s $^{-1}$ for 2015 and 0.08 \pm 0.04 m³ s $^{-1}$ for 2016. Drawdown of the upstream reservoir for repairs between the 2015 and 2016 seasons was responsible for the variability of the annual inflow rates to FCR and resulted in mean residence times of 127 \pm 116 (1 S.D.) days for 2015, and 46 \pm 23 days in 2016 (Appendix III, Fig. 1).

3.2. Temperature and oxygen profiles

3.2.1. 2015 MOM development

Near-continuous operation of the HOx with pulses from the EM successfully regenerated MOMs after each EM mixing event while maintaining thermal stratification in FCR (Fig. 2). Two MOMs developed during the 2015 monitoring period, one that lasted from 8 to 22 June and one that lasted from 1 July to fall turnover on 5 October (Fig. 2B). During the development of the first MOM, DO concentrations at 5 m (the depth of the center of the MOM) decreased by 0.12 mg L^{-1} d⁻¹, resulting in a DO concentration in the MOM on 22 June that was >7 mg L⁻¹ lower than volume-weighted DO concentrations in either the epilimnion above or the hypolimnion below. The 48 h EM activation on 22-24 June (Table 2) initially disrupted the MOM (Fig. 2B), however, a second MOM rapidly re-formed at 5 m four days after the EM activation. This MOM exhibited a mean DO concentration of 0.7 \pm 0.3 (1 S.D.) $mg L^{-1}$ and extended horizontally upstream from the dam to the inflow throughout the length of the reservoir (Fig. 3A, B). No further EM events occurred in 2015 and the second MOM that developed persisted until turnover disrupted the water column on 5 October.

The epilimnion and hypolimnion remained well-oxygenated in 2015. After the HOx was activated on 5 May, the hypolimnion maintained preseason DO concentrations, except for a short period when the HOx was temporarily deactivated during 1 June to 8 June 2015 (Table 2). After the HOx was activated again on 8 June, DO at 9 m was replenished and exhibited a mean concentration of 8.4 \pm 0.3 mg L^{-1} until the end of the season (Fig. 2B). Similar to the hypolimnion, FCR's epilimnion was never depleted of DO in the 2015 season and remained above 6.3 mg L^{-1} the whole season.

3.2.2. 2016 MOM development

Four sequential MOMs formed as a result of HOx and EM operation during the 2016 season. After the HOx had been activated on 18 April, a weak MOM developed between 3.8 and 5 m that persisted until 30 May (Fig. 2D), the same day we activated the EM (Table 2). Immediately after the EM was deactivated, DO concentrations at 5 m decreased and a second MOM developed that persisted until 26 June, with a minimum DO concentration of 4.8 mg $\rm L^{-1}$ (Fig. 2D). The EM was activated again on 26 June (Table 2) to generate a larger DO gradient between the metalimnion and other layers. DO concentrations at 5 m immediately decreased after the second EM deactivation, forming a MOM that became anoxic within 14 days and persisted for one month. The EM was activated a third time on 24 July, and after deactivation DO

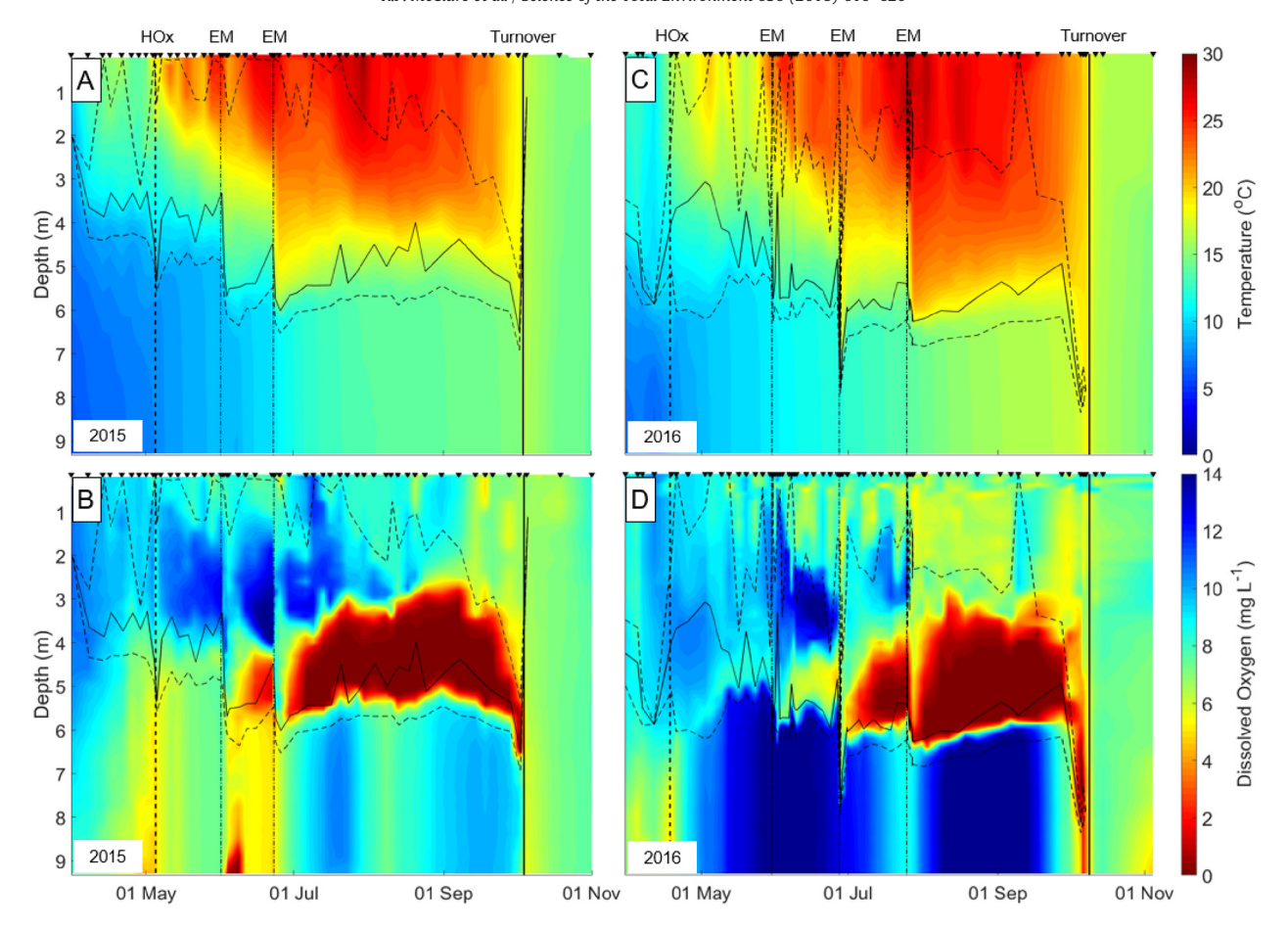


Fig. 2. Depth profiles of temperature (A, C) and dissolved oxygen concentrations (B, D) during the sampling periods in 2015 and 2016, respectively. In each figure, the thermocline depth is represented by the solid black line, while the dotted black lines represent the top and bottom depths of the metalimnion during the summer stratified period. The black triangles at the top of the figures indicate sampling days when depth profiles were collected; the remaining temperature and DO data are interpolated. The black dotted vertical lines represent when the hypolimnetic oxygenation system (HOx) and epilimnetic mixer (EM) were activated and the solid black lines represent seasonal turnover.

concentrations again decreased and an anoxic MOM developed within ten days. The final MOM remained anoxic between 3.8 and 6.2 m depth for 57 days and extended horizontally upstream from the dam to the inflow (Fig. 3B) until fall turnover on 9 October (Fig. 2D).

Hypolimnetic and epilimnetic DO concentrations remained elevated during the 2016 season (Fig. 2D). The HOx was activated on 18 April (Table 2) in 2016 and DO concentrations at 9 m depth were \geq 7.2 mg L⁻¹ the entire season. In 2016, the HOx system was never deactivated for repairs and remained operational through fall turnover. Similar to 2015, the epilimnion was never depleted of DO in the 2016 season and remained above 6.6 mg L⁻¹ (Fig. 2D).

3.3. Water column GHG dynamics

3.3.1. 2015 Dissolved CH₄ dynamics

Elevated concentrations of CH₄ in the MOMs were observed in both seasons, resulting in substantial variation in the CH₄ depth profiles (Fig. 3B, D; Fig. 4). In 2015, CH₄ concentrations at 5 m remained \leq 0.19 μ M during the first MOM. However, after the second MOM became anoxic on 6 July, CH₄ concentrations at 5 m increased by 4.4 μ M d⁻¹, reaching the highest observed CH₄ concentration in the water column (75 μ M) on 31 August. The gradient in CH₄ concentrations throughout the water column on 31 August was large: CH₄ concentrations in the metalimnion were ~24× and ~120× greater than in the epilimnion and hypolimnion, respectively. Over the next four weeks, CH₄ concentrations within the MOM remained between 47 and 75 μ M until mid-September. CH₄ concentrations at 5 m declined from 72 μ M to 6.4 μ M between 14 and 28 September and continued to decline until 5 October,

the day of fall turnover. After turnover, CH_4 concentrations at 5 m were $< 0.2 \mu M$ through the end of the 2015 monitoring period.

CH₄ concentrations remained low in the hypolimnion and epilimnion in comparison to concentrations in the MOM (Fig. 4A). The HOx maintained oxic conditions in the hypolimnion for a majority of the 2015 season, resulting in CH₄ concentrations \leq 0.3 μ M. CH₄ concentrations in the epilimnion also remained low throughout most of the monitoring period. However, there was one substantial increase in epilimnetic CH₄ on 14 September 2015, the same day when the highest CH₄ concentration was observed in the metalimnion. On this sampling day, which also coincided with elevated winds up to 9.5 m s⁻¹ but no precipitation (Fig. 5), CH₄ concentrations at 0.1 m increased from 0.2 μ M to 4.2 μ M. After turnover on 5 October 2015, CH₄ concentrations throughout the water column decreased to \leq 1.0 μ M.

3.3.2. 2016 Dissolved CH₄ dynamics

CH₄ accumulated in the MOM again in 2016, exhibiting slightly higher concentrations than in 2015. No detectable CH₄ accumulated in the first and second MOMs that developed in May and June (Fig. 3C). However, after the third MOM became anoxic on 11 July, CH₄ concentrations increased by 0.27 μ M d⁻¹, reaching 3.5 μ M by 24 July. When the fourth MOM became anoxic, CH₄ concentrations at 6.2 m increased rapidly by 3.3 μ M d⁻¹ and peaked at the highest observed concentration over both years on 9 September (128 μ M; Fig. 4C). The peak MOM CH₄ concentration in 2016 was 1.7-fold higher than the peak CH₄ concentration in the MOM on 14 September 2015. CH₄ concentrations in the MOM remained between 53 and 128 μ M until FCR turned over on 9

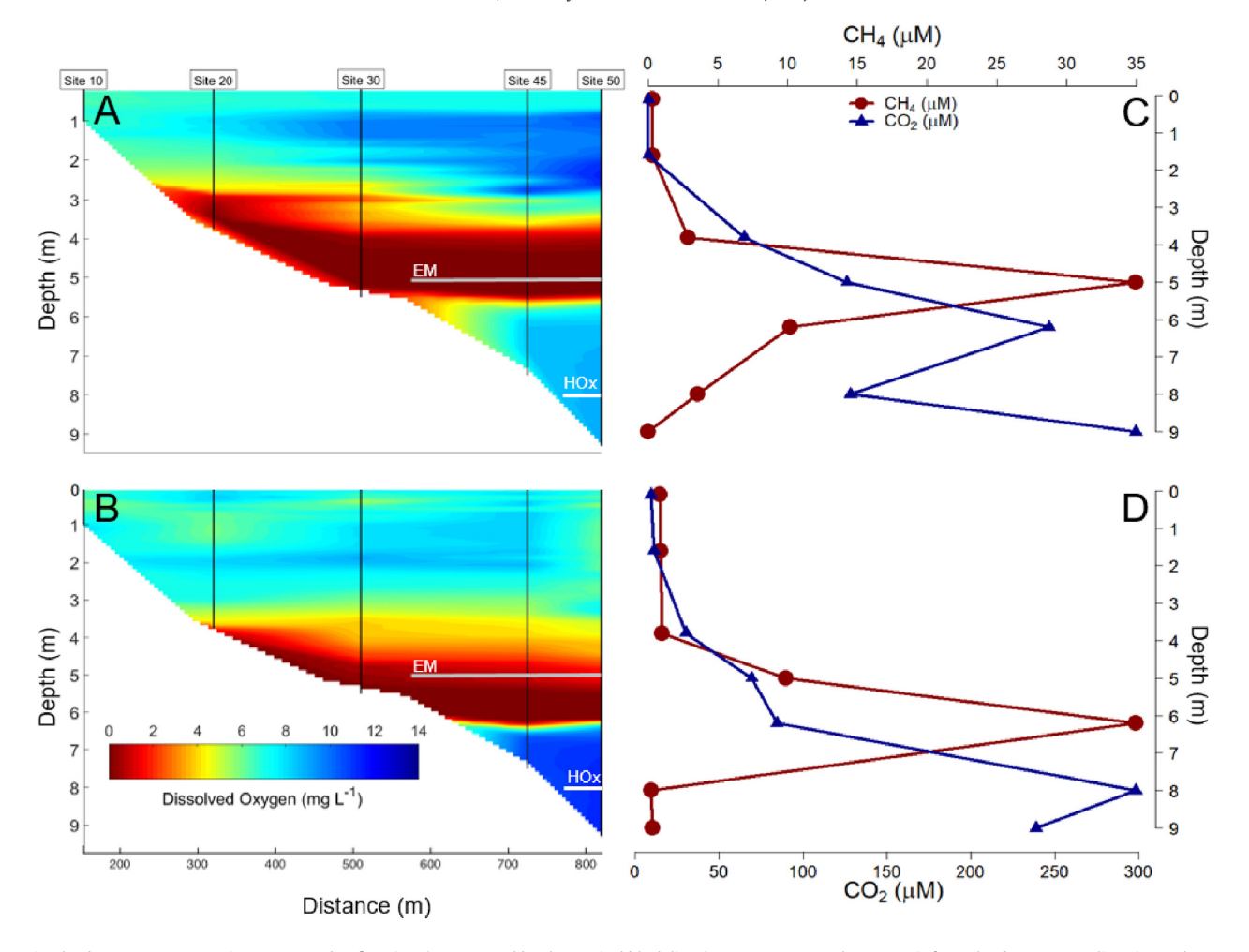


Fig. 3. Dissolved oxygen concentrations measured at five sites (represented by the vertical black lines) on a transect up the reservoir from the deepest sampling site to the upstream tributary on two select dates (see Fig. 1 map): (A) 24 August 2015, after the MOM became well-established at sites 45 and 50 and extended up the reservoir; and (B) 26 August 2016, showing the final MOM of 2016. Data between the sampling sites were linearly interpolated, and thus are not to the scale of the bathymetry map in Fig. 1. Vertical profiles from site 50 of dissolved CH₄ and CO₂ represent the water column profiles from (C) 24 August 2015 and (D) 26 August 2016.

October, after which concentrations remained $<0.2 \mu M$ in the water column for the remainder of the monitoring period.

During the 2016 season, CH₄ concentrations in the epilimnion and the hypolimnion remained <1.0 and 38 μ M, respectively, and no substantial CH₄ increases in the epilimnion were observed in the late summer, unlike in 2015. Like most of the 2015 season, epilimnetic CH₄ concentrations remained ≤1 μ M throughout the 2016 season. However, the maximum CH₄ concentrations at the sediments in 2016 were elevated compared to 2015, from 0.3 μ M in 2015 to 38 μ M in 2016.

3.3.3. 2015 Dissolved CO₂ dynamics

In comparison to elevated CH₄ concentrations in the MOM, CO₂ concentrations were highest in the oxygenated hypolimnion (Fig. 4B, D). When the HOx was activated on 5 May 2015, CO₂ concentrations at 9 m steadily increased throughout the summer stratified period and peaked at 793 μ M on 21 September. CO₂ concentrations at 9 m then remained elevated (674–793 μ M) until fall turnover on 5 October, after which CO₂ in the hypolimnion decreased rapidly. Within two weeks after turnover, CO₂ at 9 m had decreased to 68 μ M and remained between 45 and 68 μ M for the rest of the monitoring period.

 CO_2 concentrations increased in both the metalimnion and epilimnion, but never reached the elevated concentrations observed in the hypolimnion. After the second MOM developed in 2015, CO_2 at 5 m increased to 476 μ M on 21 September before fall turnover, after which CO_2 concentrations decreased to <90 μ M through 7 December (Fig. 4B). Epilimnetic CO_2 concentrations at 0.1 m remained \leq 37 μ M

during the development of both MOMs early in the season, and then exhibited two elevated peaks in the late season, one on 14 September – the same day as the peak in epilimnetic CH₄ – and another during turnover on 5 October. After turnover, CO₂ concentrations at 0.1 m remained ≥45 µM for the rest of the monitoring period.

3.3.4. 2016 Dissolved CO₂ dynamics

 CO_2 concentrations again were highest near the sediments in 2016, but were lower than 2015. After the HOx was activated in April 2016, CO $_2$ concentrations at 9 m increased at a constant rate to 112 μM within 33 days of operation. Between 25 May and 27 July, CO $_2$ concentrations ranged between 112 and 202 μM and then increased over the next 32 days at a rate of ~4.6 μM d $^{-1}$ before peaking at 330 μM on 30 September, ~52% lower than CO $_2$ concentrations in 2015. CO $_2$ concentrations at 9 m remained elevated until fall turnover on 9 October, after which CO $_2$ in the hypolimnion decreased rapidly. By 14 October, CO $_2$ at 9 m had decreased to 26 μM and remained between 26 and 12 μM for the rest of the monitoring period.

CO₂ dynamics in the metalimnion and epilimnion during 2016 exhibited largely the same patterns observed in 2015. When the HOx was activated in 2016, CO₂ in the bottom of the MOM (6.2 m) increased at a rate of 1.5 μ M d⁻¹, reaching a peak of 327 μ M on 30 September (Fig. 4D). Epilimnetic CO₂ concentrations at 0.1 m were \leq 24 μ M during the development of the first two MOMs early in the season, and then experienced two elevated peaks, one during the final EM activation (27 July) and the second at fall turnover (9 October). Epilimnetic CO₂

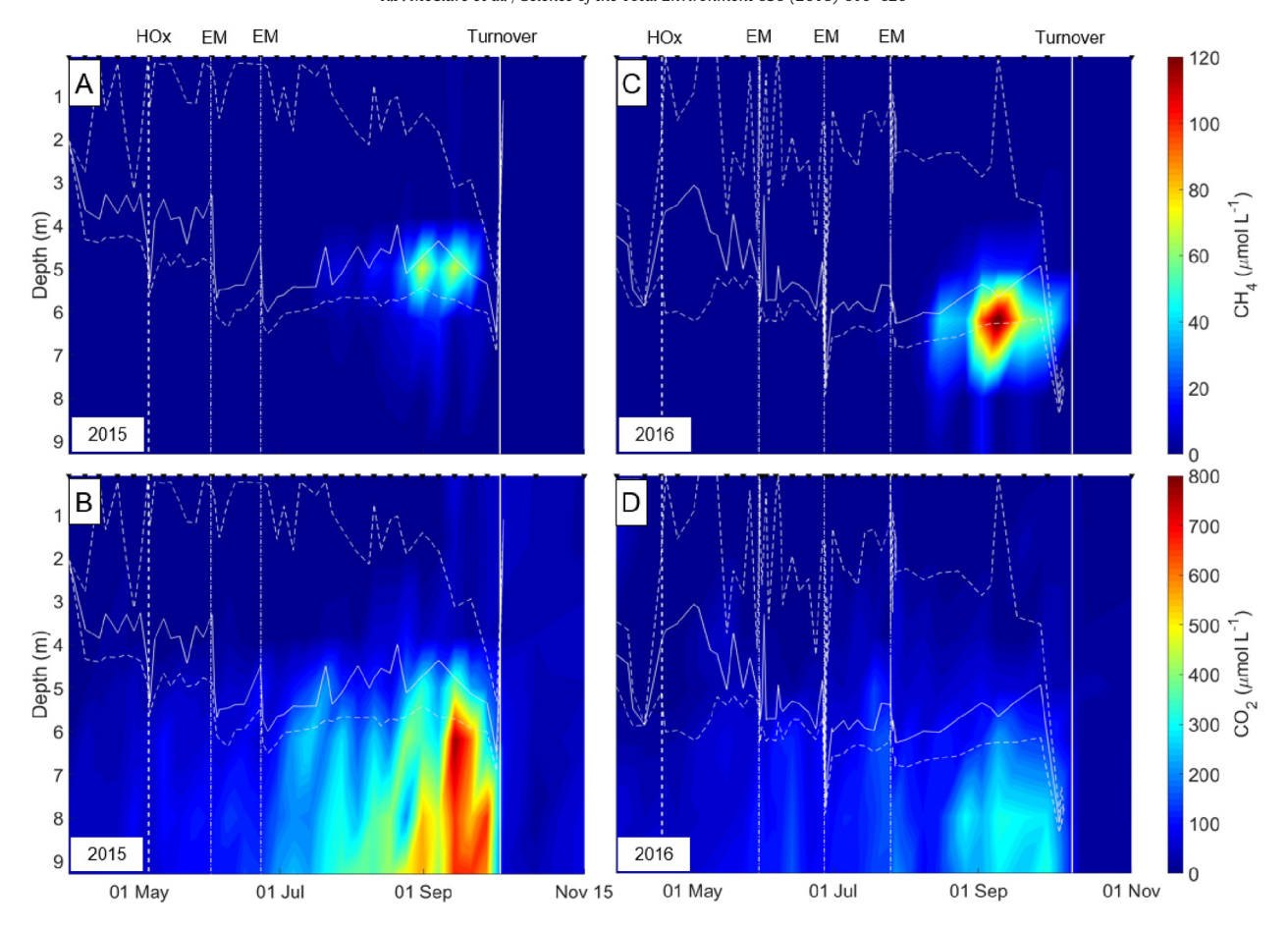


Fig. 4. Depth profiles of CH_4 (A, C) and CO_2 (B, D) during the 2015 and 2016 sampling periods. The thermocline depth is represented by the solid white line and the dotted white lines represent the top and bottom depths of the metalimnion. The black triangles at the top of the figure indicate sampling days when water sample profiles were collected; the remaining CO_2 and CH_4 data are interpolated. The black dotted vertical lines represent when the hypolimnetic oxygenation system (HOx) and epilimnetic mixer (EM) were activated and the solid black lines represent seasonal turnover.

concentrations increased by 2.1 μM d $^{-1}$ during the final EM (24–28 July) and peaked at 14 μM . During turnover, epilimnetic CO₂ concentrations increased by 2.5 μM d $^{-1}$ and peaked at 19 μM . After turnover, CO₂ concentrations at 0.1 m remained \geq 12 μM through the rest of the monitoring period.

3.4. Diffusive CH₄ and CO₂ effluxes

3.4.1. 2015 Diffusive CH₄ and CO₂ effluxes

FCR was consistently a source of CH₄ to the atmosphere via diffusive efflux both years, with the highest atmospheric exchange of CH₄ occurring on 14 September 2015, two weeks after the MOM reached its peak CH₄ concentration (Fig. 4A) and three weeks before fall turnover (Fig. 5). The highest observed CH₄ efflux on 14 September was likely due to an elevated concentration of CH4 at 0.1 m and elevated wind speeds (Fig. 5A). Efflux rates decreased to <1 mmol CH₄ m⁻² d⁻¹ by 21 September, which coincided with decreased CH₄ concentrations in the water column. However, FCR remained thermally stratified for three additional weeks after the large diffusive CH₄ efflux (Fig. 5B). Turnover in 2015 was likely initiated by a second large storm that occurred between 2 and 4 October, with an accumulated precipitation of 20 mm of rain during those 3 days and average daily wind speeds wind speeds up to 10 m s⁻¹. However, there was no substantial diffusive CH4 efflux observed during turnover or during any of the EM mixing events in 2015.

Unlike for CH_4 , FCR fluctuated between a CO_2 source and sink in 2015. CO_2 was initially a source to the atmosphere between 7 April and 5 May 2015, as thermal stratification set up. FCR then became a

 CO_2 sink (negative efflux) from 5 May until 14 September and then shifted back to a CO_2 source (positive efflux) on 14 September (Fig. 5B). Between 7 and 14 September diffusive effluxes substantially increased, from -4.57 to 135 mmol CO_2 m $^{-2}$ d $^{-1}$. The elevated CO_2 flux observed on 14 September was the second highest efflux of CO_2 observed during the two-year monitoring period and was coincident with the peak diffusive CH_4 efflux. Diffusive CO_2 efflux rates remained elevated during the following five weeks, and peaked on the day of fall turnover (Fig. 5B). The three EM events in 2015 had no detectable effects on diffusive CO_2 effluxes.

3.4.2. 2016 Diffusive CH_4 and CO_2 effluxes

The peak diffusive CH₄ efflux in 2016 again occurred prior to turnover, though its magnitude was much lower than in 2015 (Fig. 5D). FCR was again consistently a source of CH₄ to the atmosphere in 2016, however, the highest diffusive CH₄ efflux occurred on 7 June, >4 months before turnover after the first EM of the 2016 season (0.7 mmol CH₄ m⁻² d⁻¹). For the rest of the season, diffusive efflux rates remained <0.7 mmol CH₄ m⁻² d⁻¹. Like 2015, there was no elevated CH₄ efflux that occurred during seasonal turnover (9 October).

Diffusive CO_2 effluxes also shifted between a source and a sink during the 2016 season. There were no substantial increases in the diffusive CO_2 effluxes during the first two EM events in 2016, but FCR changed from a CO_2 sink to a source during the third EM. The day before the third EM (24 July), the diffusive efflux sink was -3.3 mmol CO_2 m⁻² d⁻¹, and after three days of EM operation (Table 2), the CO_2 diffusive flux had increased to 7.7 mmol CO_2 m⁻² d⁻¹. Within one week, CO_2 efflux had become negative and FCR remained a sink until 6 October,

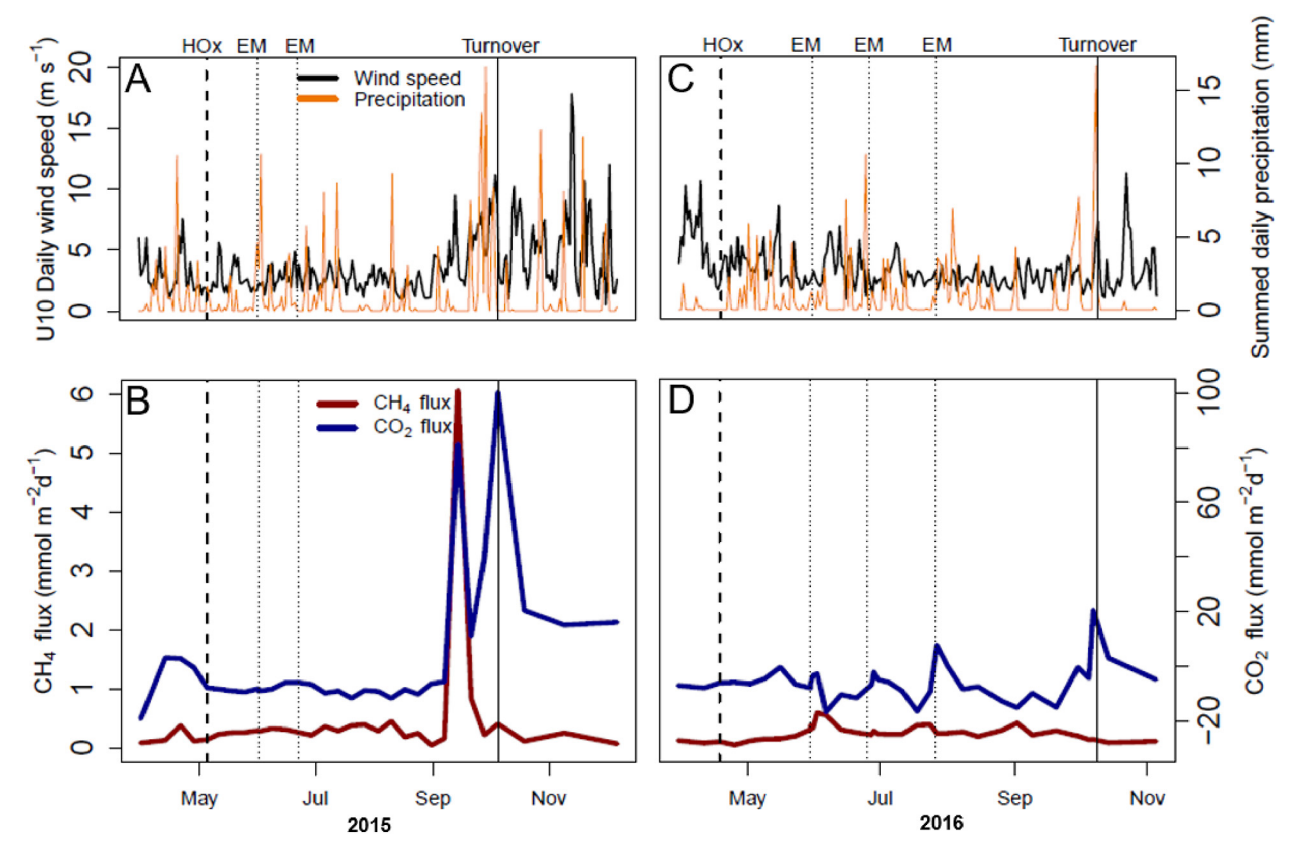


Fig. 5. Mean CH₄ (dark red) and CO₂ (blue) diffusive gas exchange rates, average daily wind speeds (black), and summed daily precipitation (orange) from 31 March to 7 December 2015 (A, B), and 30 March to 5 November 2016 (C, D). Note the difference in y-axes between panels A vs. C and B vs. D. The black dotted vertical lines represent when the hypolimnetic oxygenation system (HOx) and epilimnetic mixer (EM) were activated and the solid black lines represent seasonal turnover. (For interpretation of the references to colour in this figure legend, the reader is referred to the web version of this article.)

three days before turnover. Between 6 and 9 October, CO_2 diffusive effluxes increased by 10 mmol CO_2 m⁻² d⁻¹, and peaked on turnover (20 mmol CO_2 m⁻² d⁻¹). The peak diffusive CO_2 effluxes in 2016 were substantially lower than the peak diffusive CO_2 effluxes in 2015.

4. Discussion

The MOMs that formed in a eutrophic drinking water reservoir over two summers had large effects on the vertical profiles of CH_4 and CO_2 in the water column. HOx and EM operation coupled with consistent seasonal thermal stratification were likely the most important contributors to the development of the MOMs, which in turn altered CH_4 and CO_2 dynamics. In both years, the highest concentrations of CH_4 in the water column were observed within the MOMs, while the highest concentrations of CO_2 were observed in the oxygenated hypolimnion (Fig. 4). Our results from FCR are in contrast to reservoirs with anoxic hypolimnia, where CH_4 generally accumulates in the hypolimnion and CO_2 in the metalimnion (Bastviken et al., 2004). The changes in CO_2 and CH_4 vertical distribution in the water column may have also influenced the phenology of the peak diffusive CH_4 and CO_2 effluxes from the surface (Fig. 5).

4.1.1. MOM effects on CH₄ and CO₂ profiles

Late summer MOMs accumulated more CH_4 in the metalimnion of FCR than early summer MOMs. This pattern may be a result of lateral entrainment of CH_4 from shallow upstream sediments, the depth of the thermocline (Fig. 3A, B), and the overall warmer temperatures in the water column later in the sampling seasons. Oxygen depletion in nutrient-rich upstream sediments of FCR likely also resulted in high rates of methanogenesis, causing an increase of CH_4 within the MOM as high CH_4 water flowed from upstream sediment sites to the deepest

sampling site. Goudsmit et al. (1997) suggests that horizontal transport of CH₄ may be faster than hydraulic residence time in smaller lakes, which supports the expectation that it would take only a few weeks for elevated CH₄-enriched water to laterally entrain from anoxic metalimnetic sediments (between sites 20 and 30 in Fig. 1; Fig. 3) to the deep sampling site despite longer residence times in FCR when the MOMs developed. The shorter mean residence time observed in 2016 may also explain why CH₄ concentrations in the MOM were higher than 2015 (Fig. 4A, C). Faster entrainment of low oxygen water from the shallow upstream sediments likely transported more CH₄ from the shallow anoxic sediments to the deep sampling site of FCR. While lateral transport of CH₄ from sediments was likely the primary source of CH₄ accumulating in the MOMs (sensu Encinas Fernández et al., 2016), some CH₄ may have also been produced in the anoxic metalimnion and oxic epilimnion (Bogard et al., 2014). Additional measurements, such as the analysis of ¹³C-CH₄ isotopes from the littoral to pelagic zones (following DelSontro et al., 2017), analysis of sediment fluxes of CH₄ and terminal electron acceptors from multiple depths, and evaluation of seasonal dissolved organic carbon and total carbon stocks are needed to determine the source of CH₄ in the MOM in FCR.

There was a very high accumulation of CO_2 in the hypolimnion of FCR during both years, especially the 2015 season, which is likely due to stimulated aerobic respiration rates via HOx operation (Carey et al., 2018). HOx operation in FCR increases the hypolimnetic oxygen demand (HOD; Gerling et al., 2014), largely by increasing rates of aerobic respiration of organic matter, resulting in CO_2 production. FCR has never been dredged, resulting in the accumulation of a substantial mass of organic C in its sediments during its ~115 years since construction (Gerling et al., 2016). This organic C can then support high rates of CO_2 production during HOx operation (Carey et al., 2018). However, the continued use of the HOx might also mineralize organic C in the

sediments faster than it can be replenished annually, which might explain why hypolimnetic CO_2 was lower in 2016 than in 2015 (Fig. 4D). Similar increases in hypolimmetic respiration rates have been observed in other reservoirs with HOx systems (Gantzer et al., 2009a; Moore et al., 1996) and the evaluation of CO_2 production in these systems is important for determining the long-term C balance of managed lentic ecosystems.

The mineralization of organic C into CO_2 from HOx operation may have substantial implications for long-term C burial in reservoirs and alter waterbody C dynamics. While FCR shifted between a CO_2 sink and a source during both seasons, the summation of CO_2 diffusive effluxes across both seasons suggest that the reservoir may be a net source of CO_2 to the atmosphere. However, we note that our monitoring period excluded several months each year, including the dynamic ice-on and ice-off periods that can account for 17% and 24% of annual CO_2 and CH_4 emissions, respectively (Denfeld et al., in press). Moreover, we were unable to sample ebullition, a major pathway of reservoir CH_4 effluxes (Deemer et al., 2016). Consequently, additional monitoring is needed to determine the long-term effects of HOx and EM operation on reservoir C storage and GHG balance.

4.1.2. Diffusive CH₄ and CO₂ efflux phenology

FCR was consistently a source of CH_4 to the atmosphere through both monitoring periods. In both years, fall turnover did not result in the highest annual peaks in diffusive CH_4 effluxes, contrary to previous studies conducted in waterbodies without MOMs (e.g., Bastviken et al., 2004). Our data suggest that the peaks in CH_4 diffusive efflux were temporally decoupled from turnover because of the presence of MOMs. The development of MOMs in the middle of the water column resulted in CH_4 accumulation closer to the water's surface than would otherwise occur if the hypolimnion was anoxic, resulting in greater sensitivity of CH_4 to surface mixing events. Consequently, MOMs could result in elevated diffusive CH_4 effluxes during the summer stratified period prior to turnover, though it is important to consider that the differences in sensitivity to storms between years suggest that other processes, such as thermal stratification and mixing, likely also affect diffusive CH_4 effluxes from reservoirs with MOMs.

Diffusive CO₂ effluxes varied between a source and sink but also peaked before turnover and became elevated again during turnover both years. The elevated pre-turnover CO₂ effluxes were likely due to a combination of the oxidation of CH₄ when the MOM mixed from strong storms in 2015 and EM events that mixed CH₄ in the MOM in 2016. During the first CO₂ peak observed in September 2015, it is likely that some of the MOM CH₄ that entrained into the epilimnion during the wind storm on 14 September oxidized into CO₂. This also occurred on 29 July 2016, when the EM was activated for 48 h to develop the final MOM of the season (Table 2), and CO₂ diffusive effluxes peaked both during and shortly after the mixing. By comparing the volumeweighted mass of CH₄ in the surface waters (0.1-1.6 m), with the volume-weighted mass of CH₄ in the MOM (3.8-5 m) on 14 September 2015, it is estimated that as much as 95% of the CH₄ in the MOM that mixed into the epilimnion was oxidized into CO_2 , which may explain why FCR reverted from a CO₂ sink to a substantial CO₂ source within one week (Fig. 5C, D).

The second peak in diffusive CO_2 effluxes from FCR coincided with turnover on both seasons. It is likely that the secondary peaks were due to mixing of CO_2 that had accumulated in the hypolimnion throughout the summer into the surface waters during turnover. Thus, the timing and magnitude of diffusive CO_2 effluxes may also be affected by the presence of MOMs. If hypolimnia remain oxic during the development of MOMs, especially in reservoirs with engineered systems like HOx, diffusive CO_2 emissions could exhibit two peaks, as was observed in FCR: one CO_2 peak from oxidized CH_4 if the MOM mixes into the epilimnion prior to turnover, and a second CO_2 peak when the whole water column is homogenized during turnover.

Both diffusive CH₄ and CO₂ effluxes were substantially lower in 2016 compared to 2015 (Fig. 5C, D). This may be a result of the difference in the depth of the metalimnion between years. In 2015, the bottom depth of the metalimnion ranged between 4 and 5 m throughout the monitoring period, while the bottom depth of the metalimnion ranged between 5 and 6.5 m in 2016 (Fig. 3). Induced EM events in other studies have shown that artificial mixing will deepen both the thermocline and lower metalimnetic boundary in waterbodies (Chen et al., 2017; Cantin et al., 2011). Deeper thermocline depths will consequently result in deeper MOMs (Chen et al., 2017, 2018), as was observed in 2016 (Fig. 4D). Thus, the deeper depth of the 2016 MOMs may have hindered surface mixing from entraining metalimnetic water, preventing CH₄ from mixing to the surface. The strength and duration of EM events in 2016 were greater compared to 2015 (Table 2), yet diffusive CH₄ and CO₂ effluxes were lower, suggesting that the wind-driven mixing events in 2015 may have had a greater effect than the EM on epilimnetic mixing and diffusive effluxes in FCR.

4.1.3. Additional important considerations

Both temporal variability in diffusive flux and limited sampling spatial coverage result in potentially large underestimates of seasonal CH₄ and CO₂ emissions (Wik et al., 2016). Although this study had limited spatial sampling resolution, the aim was to capture a high temporal resolution of CH₄ and CO₂ dynamics in the water column while using engineered water quality systems to generate MOMs over two seasons. The peak diffusive CH₄ effluxes that preceded turnover in both 2015 and 2016 were likely in part a result of the MOM development and the depths at which the MOMs formed. The accumulation of CH₄ in the MOMs and not in the hypolimnion suggests that high temporal frequency sampling for CH₄ and CO₂ concentrations throughout the water column is critically important for reservoirs with engineered systems to improve water quality, because infrequent monitoring at only the surface can underestimate diffusive CH₄ and CO₂ effluxes if they are accumulating at unique sub-surface depths in the water column (such as in MOMs).

Although CH_4 and CO_2 were measured at only one sampling site in FCR, weekly CTD profiles collected at four upstream sites (Fig. 3A, B) demonstrated that the MOMs extended throughout the reservoir, suggesting that CH_4 and CO_2 dynamics at the deepest site may be representative of upstream conditions. The development of two prominent MOMs in 2015 and three MOMs in 2016, and the observed metalimnetic concentrations of CH_4 , along with the CO_2 observed in the oxygenated hypolimnion, strongly support that MOMs alter both the vertical profile of dissolved CH_4 and CO_2 in the water column and may change the timing of diffusive CH_4 and CO_2 effluxes to the atmosphere.

4.1.4. Engineered water-quality systems and reservoir C dynamics

This study investigated the effects of engineered systems designed for water quality management on reservoir CH₄ and CO₂ dynamics. As noted above, it cannot be concluded from these data that the use of HOx and EM engineered systems will exacerbate reservoir GHG emissions. Instead, the current study was designed to explore how these systems might influence seasonal CH₄ and CO₂ dynamics. As one of the first studies to our knowledge that examines the effects of water quality management systems on GHGs, our work provides a foundation for future applications. For example, HOx systems could be used to study the effects of oxygen on organic C burial at the whole-ecosystem scale. In conjunction, the use of the EM can also be used to simulate large storms, which are expected to increase in many regions (Prein et al., 2017) that can affect thermal stratification and GHG fluxes. Thus, while the design of HOx and EM systems are primarily designed for improving water quality, we suggest that they may be used to further study the role of lakes and reservoirs in the global C cycle.

5. Conclusions

Experimentally-derived MOMs from HOx and EM operation accumulated CH_4 in the metalimnion and CO_2 in the well-oxygenated hypolimnion in FCR, creating a dissolved GHG profile pattern that contrasts with observations from waterbodies without MOMs. The MOMs caused CH_4 to accumulate in the water column closer to the surface instead of at the sediments, and potentially was the cause of peak diffusive GHG emissions before seasonal turnover. Consequently, increases in both global reservoir construction and the use of engineered systems in those reservoirs to improve drinking water quality may result in an increased occurrence of MOMs, which in turn may change seasonal CH_4 and CO_2 dynamics.

Conflicts of interest

None.

Contributions

CCC conceived the original research project, from which RPM and CCC worked closely together to develop the research ideas addressed in this paper. RPM led the overall synthesis and interpretation of the data and writing with many contributions from CCC, KDH, and MES. RPM, ZWM, KDH, SC, MEL, and CCC collected field data; BRN developed new methods critical for data analysis; and RPM, BRN, ZWM, SC, MEL, and CCC compiled and analyzed data. All authors approved the final version of the manuscript.

Acknowledgements

We thank the staff at the Western Virginia Water Authority for their long-term support, especially C. Brewer, J. Morris, J. Booth, G. Belcher, B. Benninger, P. Martin, and G. Robertson. We are grateful for help with sample and data collection from J. Doubek, A. Gerling, C. Harrell, M. Ryan, and S. Klepatzki. P. Gantzer and M. Mobley provided critical help in the field with the HOx and EM systems. We are also grateful for the Virginia Tech Stream Team and the Virginia Tech Reservoir Group for their valuable comments throughout the project. This work was financially supported by the National Science Foundation CNS-1737424, DEB-1753639, Virginia Tech Dept. of Biological Sciences, the Institute for Critical Technology and Applied Science, the Fralin Institute of Life Sciences, the Virginia Tech Global Change Center, and National Fish & Wildlife Foundation Grant 13014.042027 to C.C.C.

Appendix A. Supplementary data

Supplementary data to this article can be found online at https://doi.org/10.1016/j.scitotenv.2018.04.255.

References

- AmeriFlux BASE Dataset. Tilden Meyers AmeriFlux US-WBW Walker Branch Watershed. http://ameriflux.lbl.gov, Accessed date: 2 February 2016. https://doi.org/10.17190/
- Bastviken, D., Cole, J., Pace, M.L., Tranvik, L.J., 2004. Methane emissions from lakes: dependence of lake characteristics, two regional assessments, and a global estimate. Glob. Biogeochem. Cycles 18 (4). https://doi.org/10.1029/2004GB002238.
- Beutel, M.W., Horne, A.J., 1999. A review of the effects of hypolimnetic oxygenation on lake and reservoir water quality. Lake Reserv. Manag. 15:285–297. https://doi.org/ 10.1080/07438149909354124.
- Bogard, M.J., Del Giorgio, P.A., Boutet, L., Chaves, M.C.G., Prairie, Y.T., Merante, A., Derry, A.M., 2014. Oxic water column methanogenesis as a major component of aquatic CH4 fluxes. Nat. Commun. 5. https://doi.org/10.1038/ncomms6350.
- Bolke, E.L., 1979. Dissolved-Oxygen Depletion and Other Effects of Storing Water in Flaming Gorge Reservoir, Wyoming and Utah. US Government Printing Office.
- Cantin, A., Beisner, B.E., Gunn, J.M., Prairie, Y.T., Winter, J.G., 2011. Effects of thermocline deepening on lake plankton communities. Can. J. Fish. Aquat. Sci. 68:260–276. https://doi.org/10.1139/F10-138.

- Carbon Dioxide Information Analysis Center. US Department of Energy, Recent Greenhouse Gas Concentrations. http://cdiac.ornl.gov/pns/current_ghg.html (Accessed 2016-02-02).
- Carey, C.C., Doubek, J.P., McClure, R.P., Hanson, P.C., 2018. Oxygen dynamics control the burial of organic carbon in a eutrophic reservoir. Limnol. Oceanogr. Let. https://doi. org/10.1002/lol2.10057.
- Chen, S., Lei, C., Carey, C.C., Gantzer, P.A., Little, J.C., 2017. A coupled three-dimensional hydrodynamic model for predicting hypolimnetic oxygenation and epilimnetic mixing in a shallow eutrophic reservoir. Water Resour. Res. 53:470–484. https://doi.org/10.1002/2016WR019279.
- Chen, S., Little, J.C., Carey, C.C., McClure, R.P., Lofton, M.E., Lei, C., 2018. Three-dimensional effects of artificial mixing in a shallow drinking-water reservoir. Water Resour. Res. 113:43–51. https://doi.org/10.1002/2017WR021127.
- Cole, J.J., Prairie, Y.T., Caraco, N.F., McDowell, W.H., Tranvik, L.J., Striegl, R.G., Melack, J., 2007. Plumbing the global carbon cycle: integrating inland waters into the terrestrial carbon budget. Ecosystems 10:172–185. https://doi.org/10.1007/s10021-006-9013-8.
- Cole, J.J., Bade, D.L., Bastviken, D., Pace, M.L., Van de Bogert, M., 2010. Multiple approaches to estimating air-water gas exchange in small lakes. Limnol. Oceanogr. Methods 8: 285–293. https://doi.org/10.4319/lom.2010.8.285.
- Deemer, B.R., Harrison, J.A., Li, S., Beaulieu, J.J., DelSontro, T., Barros, N., Bezerra-Neto, J.F., Powers, S.M., dos Santos, M.A., Vonk, J.A., 2016. Greenhouse gas emissions from reservoir water surfaces: a new global synthesis. Bioscience 66:949–964. https://doi.org/ 10.1093/biosci/biw117.
- DelSontro, T., del Giorgio, P.A., Prairie, Y.T., 2017. No longer a paradox: the interaction between physical transport and biological processes explains the spatial distribution of surface water methane within and across lakes. Ecosystems:1–15 https://doi.org/10.1007/s10021-017-0205-1.
- Denfeld, B.A., Baulch, M.A., del Giorgio, P.A., Hampton, S.E., Karlson, J., 2018. A synthesis of carbon dioxide and methane dynamics during ice-covered period of northern lakes. Limnol. Oceanogr. Lett. https://doi.org/10.1002/lol2.10079 (in press).
- Downing, J.A., Prairie, Y.T., Cole, J.J., Duarte, C.M., Tranvik, L.J., Striegl, R.G., McDowell, W.H., Kortelainen, P., Caraco, N.F., Melack, J.M., Middelburg, J.J., 2006. The global abundance and size distribution of lakes, ponds, and impoundments. Limnol. Oceanogr. 51: 2388–2397. https://doi.org/10.4319/lo.2006.51.5.2388.
- Dugan, H.A., Woolway, R.I., Santoso, A.B., Corman, J.R., Jaimes, A., Nodine, E.R., Patil, V.P., Zwart, J.A., Brentrup, J.A., Hetherington, A.L., Oliver, S.K., 2016. Consequences of gas flux model choice on the interpretation of metabolic balance across 15 lakes. Inland Waters. 6:581–592. https://doi.org/10.5268/IW-6.4.836.
- Effler, S.W., Gelda, R.K., Perkins, M., Matthews, D.A., Owens, E.M., Stepczuk, C., Bader, A.P., 1998. Characteristics and origins of metalimnetic dissolved oxygen minima in a eutrophic reservoir. Lake Res. Mgmt. 14:332–343. https://doi.org/10.1080/ 07438149809354341.
- Encinas Fernández, J., Peeters, F., Hofmann, H., 2016. On the methane paradox: transport from shallow water zones rather than in situ methanogenesis is the major source of CH₄ in the open surface water of lakes. J. Geophys. Res. Biogeosci. 121:2717–2726. https://doi.org/10.1002/2016[G003586.
- Gantzer, P.A., Bryant, L.D., Little, J.C., 2009. Effect of hypolimnetic oxygenation on oxygen depletion rates in two water-supply reservoirs. Water Res. 43:1700–1710. https:// doi.org/10.1016/j.watres.2008.12.053.
- Gerling, A.B., Browne, R.G., Gantzer, P.A., Mobley, M.H., Little, J.C., Carey, C.C., 2014. First report of the successful operation of a side stream supersaturation hypolimnetic oxygenation system in a eutrophic, shallow reservoir. Water Res. 67:129–143. https:// doi.org/10.1016/j.watres.2014.09.002.
- Gerling, A.B., Munger, Z.W., Doubek, J.P., Hamre, K.D., Gantzer, P.A., Little, J.C., Carey, C.C., 2016. Whole-catchment manipulations of internal and external loading reveal the sensitivity of a century-old reservoir to hypoxia. Ecosystems 19:555–571. https:// doi.org/10.1007/s10021-015-9951-0.
- Goudsmit, G.H., Peeters, F., Gloor, M., Wüest, A., 1997. Boundary versus internal diapycnal mixing in stratified natural waters. J. Geophys. Res. 102, 27,903–27,914.
- Hudson, Felisa, May 2004. RSKSOP-175, Revision No. 2.
- Joehnk, K.D., Umlauf, L., 2001. Modelling the metalimnetic oxygen minimum in a medium sized alpine lake. Ecol. Model. 136:67–80. https://doi.org/10.1016/S0304-3800(00) 00381-1
- Kreling, J., Bravidor, J., Engelhardt, C., Hupfer, M., Koschorreck, M., Lorke, A., 2017. The importance of physical transport and oxygen consumption for the development of a metalimnetic oxygen minimum in a lake. Limnol. Oceanogr. 62:348–363. https://doi.org/10.1002/lno.10430.
- Liboriussen, L., Søndergaard, M., Jeppesen, E., Thorsgaard, I., Grünfeld, S., Jakobsen, T.S., Hansen, K., 2009. Effects of hypolimnetic oxygenation on water quality: results from five Danish lakes. Hydrobiologia 625:157–172. https://doi.org/10.1007/s10750-009-9705-0.
- Moore, B.C., Chen, P.H., Funk, W.H., Yonge, D., 1996. A model for predicting lake sediment oxygen demand following hypolimnetic aeration. J. Am. Water Resour. Assn. 32: 723–731. https://doi.org/10.1111/j.1752-1688.1996.tb03469.x.
- Munger, Z.W., Carey, C.C., Gerling, A.B., Hamre, K.D., Doubek, J.P., Klepatzki, S.D., McClure, R.P., Schreiber, M.E., 2016. Effectiveness of hypolimnetic oxygenation for preventing accumulation of Fe and Mn in a drinking water reservoir. Water Res. 106:1–14. https://doi.org/10.1016/j.watres.2016.09.038.
- Musenze, R.S., Grinham, A., Werner, U., Gale, D., Sturm, K., Udy, J., Yuan, Z., 2014. Assessing the spatial and temporal variability of diffusive methane and nitrous oxide emissions from subtropical freshwater reservoirs. Environ. Sci. Technol. 48:14499–14507. https://doi.org/10.1021/es505324h.
- Prein, A.F., Rasmussen, R.M., Ikeda, K., Liu, C., Clark, M.P., Holland, G.J., 2017. The future intensification of hourly precipitation extremes. Nat. Clim. Chang. 7:48–52. https://doi.org/10.1038/nclimate3168.

- R Development Core Team, 2016. R Foundation for Statistical Computing. Vienna, Austria. http://r-project.org.
- Rasilo, T., Prairie, Y.T., Giorgio, P.A., 2015. Large-scale patterns in summer diffusive CH₄ fluxes across boreal lakes, and contribution to diffusive C emissions. Glob. Chang. Biol. 21:1124–1139. https://doi.org/10.1111/gcb.12741.
- Read, J.S., Hamilton, D.P., Jones, I.D., Muraoka, K., Winslow, L.A., Kroiss, R., Wu, C.H., Gaiser, E., 2011. Derivation of lake mixing and stratification indices from high-resolution lake buoy data. Environ. Model. Softw. 26:1325–1336. https://doi.org/10.1016/j.envsoft.2011.05.006.
- Sander, R., 2015. Compilation of Henry's law constants (version 4.0) for water as solvent. Atmos. Chem. Phys. 15:4399–4981, https://doi.org/10.5194/acp-15-4399-2015.
- Shapiro, J., 1960. The cause of a metalimnetic minimum of dissolved oxygen. Limnol. Oceanogr. 5:216–227. https://doi.org/10.4319/lo.1960.5.2.0216.
- Singleton, V.L., Rueda, F.J., Little, J.C., 2010. A coupled bubble plume-reservoir model for hypolimnetic oxygenation. Water Resour. Res. 46. https://doi.org/10.1029/ 2009WR009012.
- Thornton, K.W., Kimmel, B.L., Payne, F.E., 1990. Reservoir Limnology: Ecological Perspectives. John Wiley & Sons.
- Tranvik, L.J., Downing, J.A., Cotner, J.B., Loiselle, S.A., Striegl, R.G., Ballatore, T.J., Kortelainen, P.L., 2009. Lakes and reservoirs as regulators of carbon cycling and climate. Limnol. Oceanogr. 54, 2298–2314 (6part2). (doi: 10.43r 19/lo.2009.54.6_part_2.2298).

- Vachon, D., Del Giorgio, P.A., 2014. Whole-lake CO₂ dynamics in response to storm events in two morphologically different lakes. Ecosystems 17:1338–1353. https://doi.org/ 10.1007/s10021-014-9799-8.
- Wanninkhof, R., 1992. Relationship between wind speed and gas exchange. J. Geophys. Res. 97:7373–7382. https://doi.org/10.1029/92JC00188. Wik, M., Thornton, B.F., Bastviken, D., Uhlbäck, J., Crill, P.M., 2016. Biased sampling of
- Wik, M., Thornton, B.F., Bastviken, D., Uhlbäck, J., Crill, P.M., 2016. Biased sampling of methane release from northern lakes: a problem for extrapolation. Geophys. Res. Lett. https://doi.org/10.1002/2015GL066501.
- Williams, N.T., 2007. Modeling Dissolved Oxygen in Lake Powell Using CE-QUAL-W2. M.S. Thesis. Brigham Young University, Provo, UT.
- Winslow, L.A., Zwart, J.A., Batt, R.D., Dugan, H.A., Woolway, R.I., Corman, J.R., Hanson, P.C., Read, J.S., 2016. LakeMetabolizer: an R package for estimating lake metabolism from free-water oxygen using diverse statistical models. Inland Waters. 6:622–636. https://doi.org/10.5268/IW-6.4.88.
- Zarfl, C., Lumsdon, A.E., Berlekamp, J., Tydecks, L., Tockner, K., 2015. A global boom in hydropower dam construction. Aquat. Sci. 77:161–170. https://doi.org/10.1007/s00027-014-0377-0.